

Experimental Determination of Ballistic Performance of Composite Material Kevlar 29 and Alumina Powder/ Epoxy by Spherical Projectile

Luay Hashem Abbud

Department of Air conditioning and Refrigeration Engineering

Mustaqbal University College

luayhashem@yahoo.com

Abstract

In this study, a response of hybrid composite laminate woven fiber Kevlar29 – Al₂O₃ Powder/ Epoxy subjected to high velocity impact loading is presented. The energy absorbed due to impact of small rigid projectile on composite materials targets is determined experimentally. The energy absorbed due to impact of hemispherical projectiles on the developed composite laminates is investigated. The results revealed the maximum ballistic limit at impact velocity is found to be 390.87 ± 6 m/s for an the 18 mm target thickness. The ballistic limit velocity predictions are based on the theoretical method presented from another article. The initial velocity and residual velocity results showed good is agreement compared with the predicted results of Ipson and Recht equations. With 5.4 % of accuracy based on the experimental value for the theoretical model for ballistic limit velocity.

Keywords: Impact and Ballistic, Al₂O₃, Laminates, Armor and Hybrid composite

المخلص

يتضمن البحث دراسة عمل مركب هجين من ليف Kevlar29 ومسحوق اوكسيد الألمنيوم و الأيوكسي لتحملها الصدمة من المقذوفات الصلدة النصف كروية ذات السرعة العالية التي تصل اقصى سرعة بالستية لها 6 ± 390.87 م/ثا لسمك مقدارة 18 ملم وان السرعة بالستية معتمدة على الجزء النظري الذي قدم من قبل باحث آخر وقد ركزت الدراسة على الطاقة الممتصة بسبب تأثير المقذوفات الصلدة على الاهداف المركبة التي حسبت بشكل تجريبي. وقد تم مقارنة نتائج السرعة الابتدائية والسرعة النهائية مع النتائج المتوقعة لمعادلة Ipson و Recht وكانت النتائج متقاربة جداً ونسبة الخطأ أكثر دقة 5.4% من القيمة التجريبية للنموذج النظري ل سرعة الحد البالستي.

الكلمات المفتاحية: الصدمة والبالستية، ألومينا، صفائح ، دروع ومواد مركبة هجينة

1. Introduction

It is only during the early years of the Industrial Revolution that improved methods of providing more armor were developed. This was mainly due to the improved production techniques and the need to overcome continuously escalating threats. For thousands of years, warfare was conducted on foot and on horseback. However, during the last sixty years, drastic changes in warfare have taken place. Introducing new materials enhanced the use of composites in personal armor. The Kevlar fibers reinforced composites were used extensively for that purpose. Helmets, armor jackets and vests as well as leg armor were made of such materials. Ballistic penetration experiments have been performed on aluminum nitride ceramic at a velocity ranging between 1000 to 1200 m/s (Yadav 2003). The proposed three types from ceramics were effected impact by using steel projectile. However, the damage was discussed and compared for the different types of ceramics (Strassburger,1994; Kozhushko,1991). The proposed finite element simulations and the experimental work during high velocity impact on confined multi-layered ceramic/steel targets (Pablo,2000,Teng,2008). The ballistic performance of Polymethylmethacrylate under impact by a rigid spherical projectile in the range of 89.3 – 670 m/s in this paper proposed analytical model for the ballistic limit velocity from the work done for target based on the experimental observations (Abbud,2010). The

experimental investigated depth of penetration and crack formation by small steel spheres projectiles of thicker armour ceramic targets under high velocity impact (Paul 1998). Sintered sub- μm Al_2O_3 was the development of highly transparent armor components of hard and high strength for thin targets components (Andreas,2005). Impact behavior of ballistic performance of various alloys aluminum 7075-T651 against 7.62 mm projectiles were conducted Increase in the hardness of the aluminum alloys led to increase in the resistance to the projectiles effectively (Teyfik, 2008). The influence of the high-velocity impact tests were have proposed the experimental work and a finite element numerical model on thin woven carbon/epoxy laminates. Also, the projectile, a steel sphere weighting 1.73 g, was launched at a velocities ranging from 70 to 531 m/s (Lopez, 2008). A finite element numerical model for the early impact behaviour of single and multi-ply Kevlars 129 fabric armour systems (Novotny,2007;Tan,2006). The fracture behaviour and damage evolution in mullite fibre reinforced–mullite matrix composites have been proposed by using chevron notch (CN) technique and ballistic impact tests (Boccaccini 2005). The energy and momentum changes were the proposed of three approaches an analytical approach, based on first principles, an analytical evolution of applying penetration prediction equations and an experimental were presented (Hetherington 1996). Several studies have been performed to determine the ballistic limit velocity by flat cylindrical, ogive and hemispherical nosed steel projectiles of 19 mm diameter of layered aluminum plates of different thicknesses (Gupta, 2008).

2. Experimental Setup

2.1 Tensile and Compression tests of the composite

An important subject for this investigation is to study the stress – strain behavior of the Kevlar fiber and Al_2O_3 / Epoxy for bi-directional woven fiber. The tensile and compression test devices are carried out by using a universal testing machine (Instron model 3366). Tensile tests are conducted according to the standard (ASTM D 3039/D 3039 M-95a) (ASTM Standards, 1995). The standard method determines the in–plane tensile properties of polymer matrix composite materials reinforced by high–modulus fiber. The displacement and applied loads recorded and the data were acquired digitally. The composite materials properties were calculated by using a composite strain gage/quarter–bridge strain gauge circuit supplied from Tokyo (Sokki Kenkyuio Co., Ltd. The utilized gage type is a BFLA – 2 – 8 with a gage resistance of $120 \pm 0.3 \Omega$. Then, the strain was connected with a Data Acquisition (DAQ) bridge system for reading the transverse strain.

2.2 High Velocity Test

High velocity tests were carried out using a high velocity testing rig. Basically, the rig consisted of a double–clamped base on which a gun barrel of (10 mm) nominal bore and (300 mm) in length was mounted as shown **Figure 1**. In the line of fire for the projectile, the velocity before the target and the residual velocity after the target were measured by high speed cameras. Other parts of the catch chamber unit are the anvil and impact base. They are important to hold the specimen to be tested, when the specimen has been placed between the base and the anvil as shown in **Figure 2**; both were tightened by using nuts and bolts to avoid the specimen moving out of the impacted targets.

2.3 Projectile velocity measurement

The projectile velocity measurement test was performed to compare between the theoretical projectile velocity and the actual projectile velocity. For each pressure setting, a similar projectile shape and mean weight was used to obtain the mean projectile muzzle

velocity. The test results are as shown in **Figure 3**. The overall results showed that the mean projectile velocities measured from the modified ballistic testing apparatus have a 12 % difference from the theoretical calculation. This was caused by the friction effect that occurs during the projectile movement inside the barrel due to any imperfections in the projectile contour. Lesions or erosion damage were found prominently at the neck and frontal section of the projectile (after recovery). Also, it was observed that the difference is significant at higher speed due to an intense friction effect.

The projectile mass is denoted by m , the length of barrel by L , and the cross-sectional area of the barrel by A . The propellant pressure at the back end of the projectile is denoted by the letter P_p . At any instant of time, Newton's law applied to the projectile as shown in equation (1) where u_p is the instantaneous projectile velocity and x_p is the corresponding distance traveled by the projectile (Seigel, 1965).

$$m \frac{du_p}{dt} = m u_p \frac{du_p}{dx_p} = p_p A \quad (1)$$

If equation (1) is integrated, it becomes as stated in equation (2) where v is the muzzle velocity of the projectile. (Seigel 1965).

$$m \frac{v^2}{2} = A \int_0^L p_p dx_p \quad (2)$$

The spatial average propelling pressure, p is defined as shown in equation (3)

$$p = \frac{1}{L} \int_0^L p_p dx_p \quad (3)$$

The projectile velocity is as shown in equation (4). (Seigel 1965).

$$v = \sqrt{\frac{2pAL}{m}} \quad (4)$$

This result, equation (4), indicates essentially the factors upon which the projectile velocity depends. To increase the projectile velocity, one must increase the value of the quantities under the square root sign. Thus, the first step in achieving a higher projectile velocity is to change the sizes of the projectile and barrel so as to increase the value of AL/m ; this requires, for a given cross-sectional area A of the barrel, that m be smaller and L larger.

3. Analytical Models

The theoretical model of the penetration and perforation of rigid projectile hemispherical against a hybrid composite (Kevlar-29, Al_2O_3 and epoxy) target plate clamped at its outer periphery will be based on the conservation of the total energy; in this case the loss of the kinetic energy of the projectile $\Delta K.E$ is equated to the total work done W_T in the deformation. The energy was assumed to be classified into three types that include (Abu Talib, 2012):

- The elastic work, W_E
- The work done radial stretching, W_s
- The work done plastic bending, W_b

The total work done is the sum of the above-mentioned individual work expressions (Abu Talib, 2012).

$$W_T = W_E + W_S + W_b \quad (5)$$

$$W_T = \frac{3\pi\sigma_y^2 h R^2}{(-c + 2b + 2a)} (1 - \nu_{21}\nu_{12}) \left(\frac{d_2}{d_2 + 2} \right) + \frac{\pi w_0 e^{-r}}{6(1 - \nu_{21}\nu_{12})} \left[\frac{E_2(-r - 1 + \nu_{21})(3h^2 + h^3) +}{E_1(1 - \nu_{12}r - \nu_{12})(3h^2 + h^3)} \right]$$

$$\frac{1}{2} m V_b^2 = \frac{3\pi\sigma_y^2 h R^2}{(-c + 2b + 2a)} (1 - \nu_{21}\nu_{12}) \left(\frac{d_2}{d_2 + 2} \right) + \frac{\pi w_0 e^{-r}}{6(1 - \nu_{21}\nu_{12})} \left[\frac{E_2(-r - 1 + \nu_{21})(3h^2 + h^3) +}{E_1(1 - \nu_{12}r - \nu_{12})(3h^2 + h^3)} \right]$$

Finally, the ballistic limit velocity V_b of the target function of its composite material properties can be expressed as: (Abu Talib, 2012)

$$V_b = \sqrt{\frac{2}{m} \left(\frac{3\pi\sigma_y^2 h R^2}{(-c + 2b + 2a)} (1 - \nu_{21}\nu_{12}) \left(\frac{d_2}{d_2 + 2} \right) + \frac{\pi w_0 e^{-r}}{6(1 - \nu_{21}\nu_{12})} \left[\frac{E_2(-r - 1 + \nu_{21})(3h^2 + h^3) +}{E_1(1 - \nu_{12}r - \nu_{12})(3h^2 + h^3)} \right] \right)} \quad (6)$$

4. Results and Discussions

4.1 Mechanical Properties of the Tensile and compression tests

The tensile tests have been applied for pure epoxy resin and aluminum oxide powder with reinforcement fibers Kevlar 29. The particle size for alumina powder is 10 μm and the weight fraction has values for all tests equal to 30 %. These tests were done at room temperature. Two types of tests are used for evaluating the mechanical properties of the composites materials, which are the tensile tests and the compression test. The stress strain curves for the tensile and compression tests are shown in **Figures 4** and **5**. The figures represent the tensile test in hybrid composite laminate woven fiber Kevlar29 – Al_2O_3 Powder / Epoxy, with a strain gauge to measure the lateral strain and the Poisson's ratio. It is clear that there is an effect of the mechanical properties of the alumina /epoxy on the overall properties for the composite ply. This effect is decreased as the properties of the fiber increase as in the stress strain for Kevlar reinforcement shown in **Figure 4**. It was shown that the Al_2O_3 / Epoxy not only gives higher properties but also give large woven factors. This is because of its higher properties. The composite properties are affected directly by the fiber properties. This causes the highest properties for the Kevlar fiber composite.

4.2 Impact Test

The impact testes are done for the fabricated specimens as shown and discussed in this section. The first parameter studied for these tests is the effect of incident velocity on the residual velocity. The second parameter is effect of aread density on ballistic limit velocity. This is clearly demonstrated in **Figure 6** in which plot for the armor composite material (Kevlar 29 + Al_2O_3 / Epoxy) against hemispherical projectile diameter 8 mm and weight 5 g. For this reason the different layers woven Kevlar reinforce and Al_2O_3 / Epoxy composite plate different thickness and 100 * 100 mm squared. The clamping reduces the dimension diameter 80 mm. The results for these tests are shown in **Figures (7 - 13)** are show that the residual velocity increased as the incident velocity increases because the residual energy is not absorbed and increases with the incident velocity for armor composite material (Kevlar 29 + Al_2O_3 / Epoxy) targets of different layers in range 3,4,6,8,10,20 and 30 layers. The comparison all figures with empirical suggested formula by Ipson and Recht (Recht,1963), the results good agreements is obtained and average percentage error is 3 %. The formula is a power function of the incident velocity and the

ballistic velocity as follows: $V_r = \sqrt{V_i^2 - V_b^2}$, where V_r is the residual velocity, V_i is the incident velocity and V_b is the ballistic velocity.

The percentage error is 5.4 % calculated based on the experimental value for the theoretical model for ballistic limit velocity V_b .

$$\text{Error \%} = \frac{V_{bth} - V_{bexp}}{V_{bexp}} \times 100\%$$

The ballistic limit velocity was a critical issue. Experimental, numerous test were conducted at hybrid composite with thickness near 18 mm to estimate the ballistic limit under shots by hemispherical projectile, and the velocity data and pressure gage data were recorded. The ballistic limit velocity for armor composite material (Kevlar29 + Al₂O₃ / Epoxy) is higher than other composite materials, which indicates these materials are capable of absorbing more energy during high impact applications, was found to be 30 layers, which indicates that this stacking sequence withstands a higher velocity and no penetration at a maximum velocity of 390.87 ± 7 m/s and therefore absorbs more energy during the impact as shown in **Table 1**.

Ballistic limit test data were recorded for full arrest with hybrid composite specimen, and the maximum energy absorption was 381.9 J at 390.87 m/s with a target thickness of 18 mm as shown in **Table 1**. Also the ballistic limit results are compared with theoretical results by calculating the ballistic velocity as expressed in equation 6.

Intrinsically, the impact depends on the shape of the projectile end and the target geometry. The area of projectile nose related to the amount of impact force concentrated in the projectile tip at the impact moment, in this predictive the failure mechanism of composite relate with projectile velocity, projectile shape criteria. Essentially, the failure mode must be clarified when the V_i is larger than the necessitous velocity for penetration, The absorbed kinetic energy increase with increasing impact velocity. Also, the amount of energy absorption is dependent on increase of layer number. **Figures (14 - 16)** are show photos of the armor composite material target woven fiber after going through the impact of hemispherical projectile for different thickness.

Conclusions

The main conclusions of that can be drawn are:

1. From the bests for determining the mechanical properties of woven fiber and alumina powder composite materials, yield stress, compression and modules elasticity were evaluated which were improvement in the performance of hybrid composites.
2. The delamination and large deformation energies are found to be increased as the incident velocity increases near the ballistic limit velocity.
3. The absorbing energy due to impact is found to be higher for hybrid composite that have the higher mechanical properties which were the increase in target thickness improves the ballistic performance of a target.

Fig.1. Ballistic panel Gas gun (Mohamed 2007)

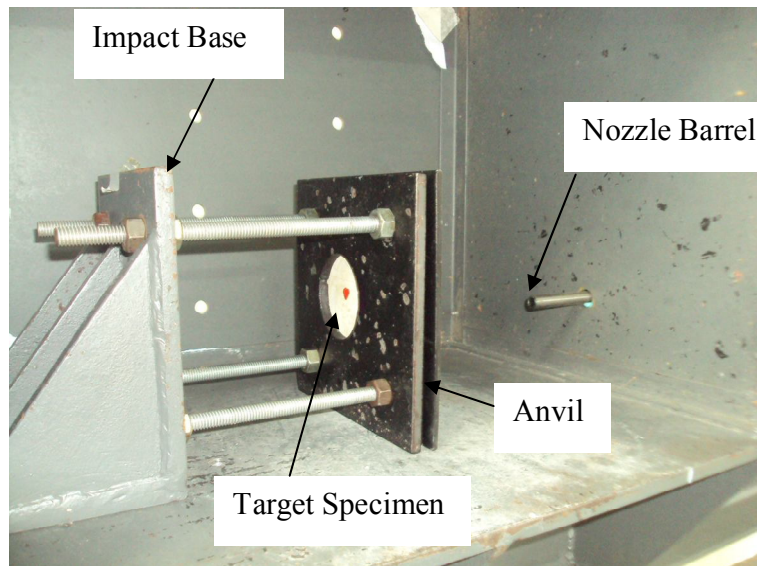


Fig. 2 The target specimen has been placed between the base and the anvil

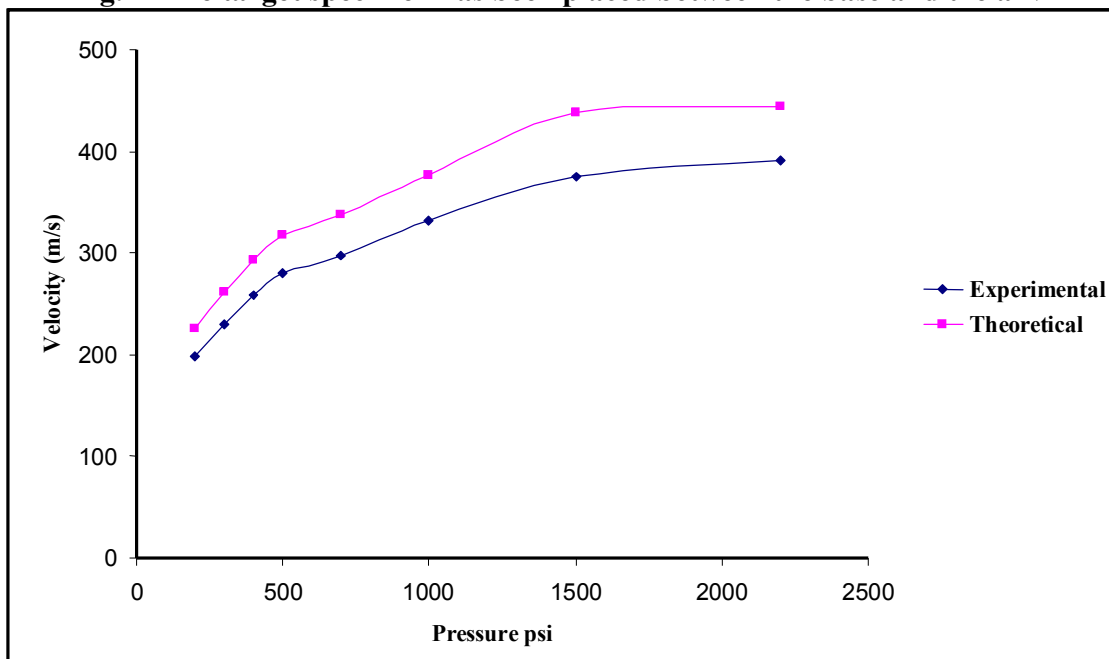


Fig. 3. Velocity measured with pressure for gas gun

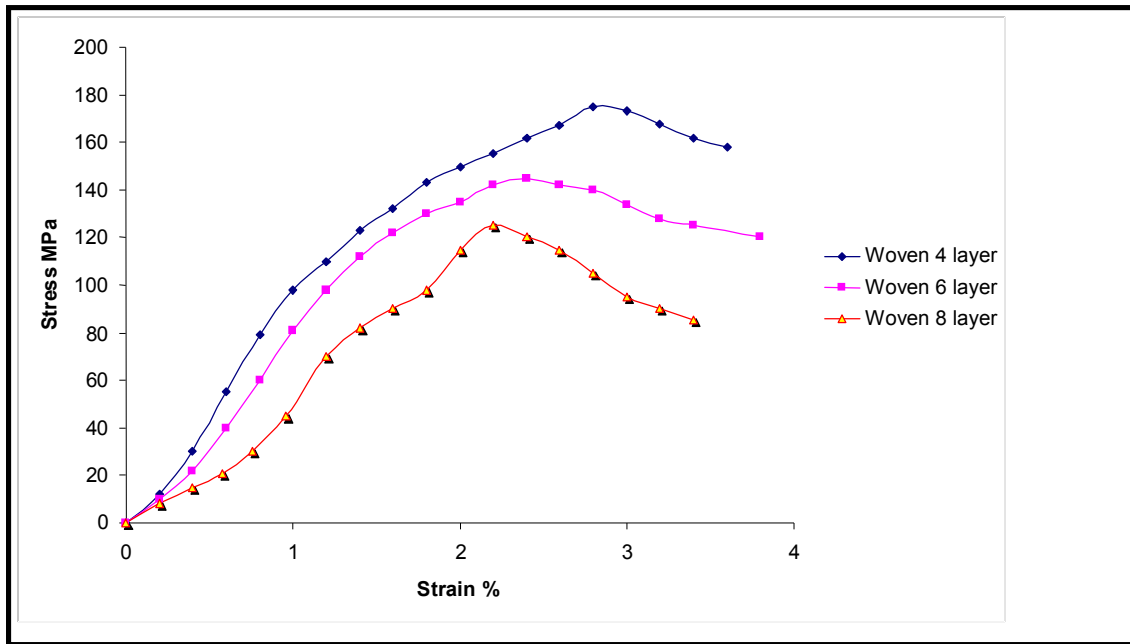


Fig. 4. Tensile stress strain for composite materials woven Kevlar

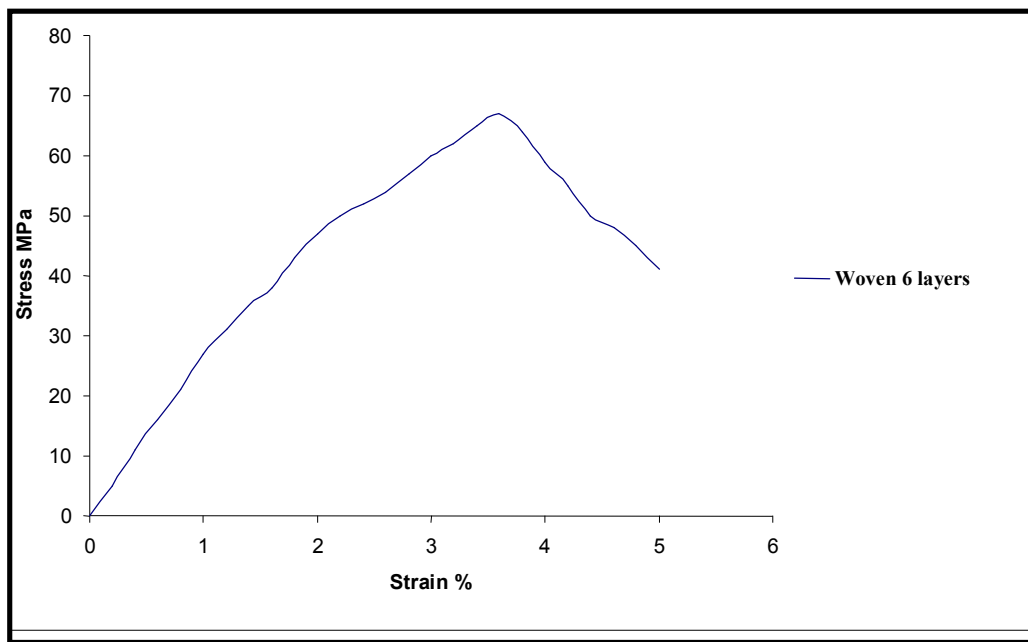


Fig 5. Compression stress strain for composite 6 layer woven Kevlar

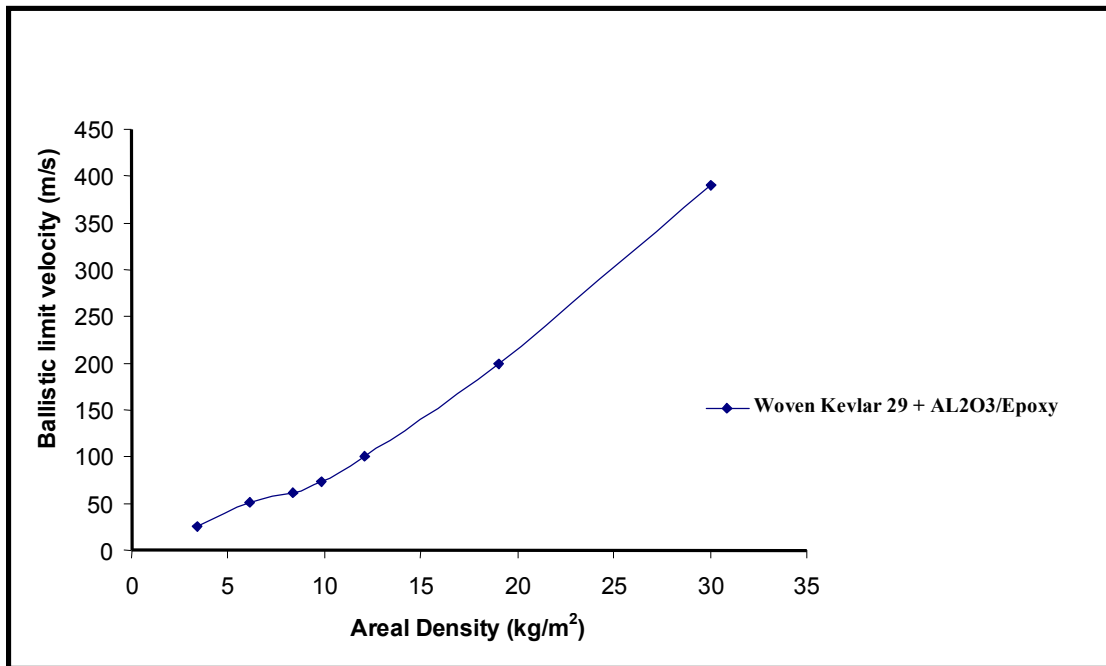


Fig. 6. Ballistic Performance of armor composite material versus areal density by hemispherical projectile

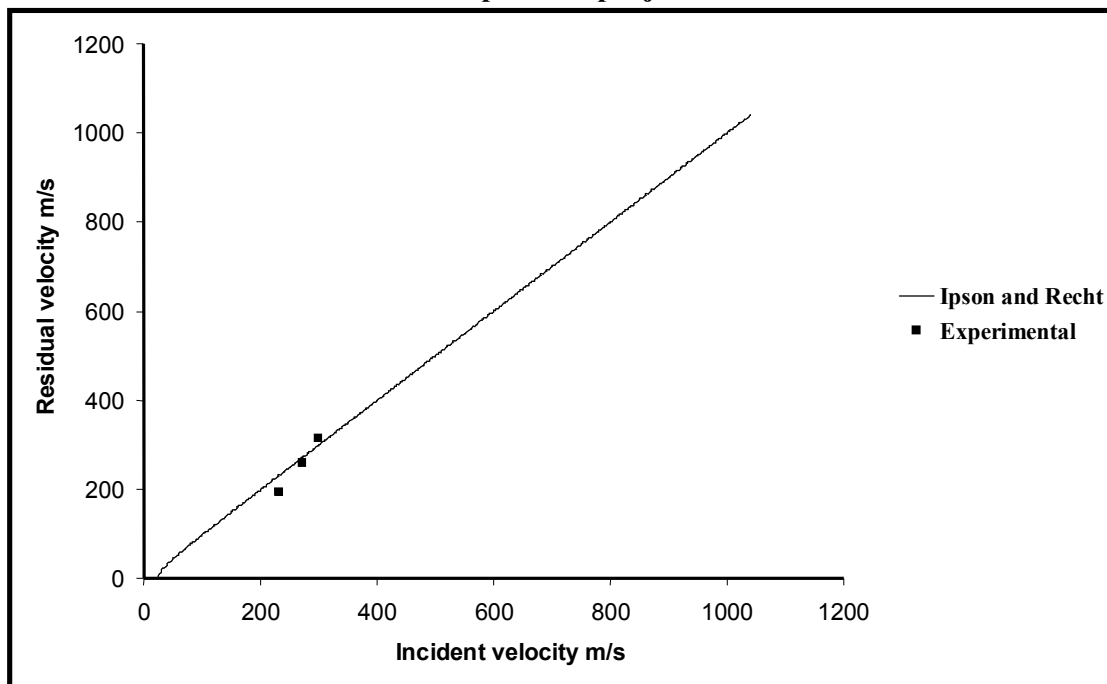


Fig. 7. Final velocity $V(r)$ versus incident velocity $V(i)$ for 3 layer woven composite by hemispherical projectile

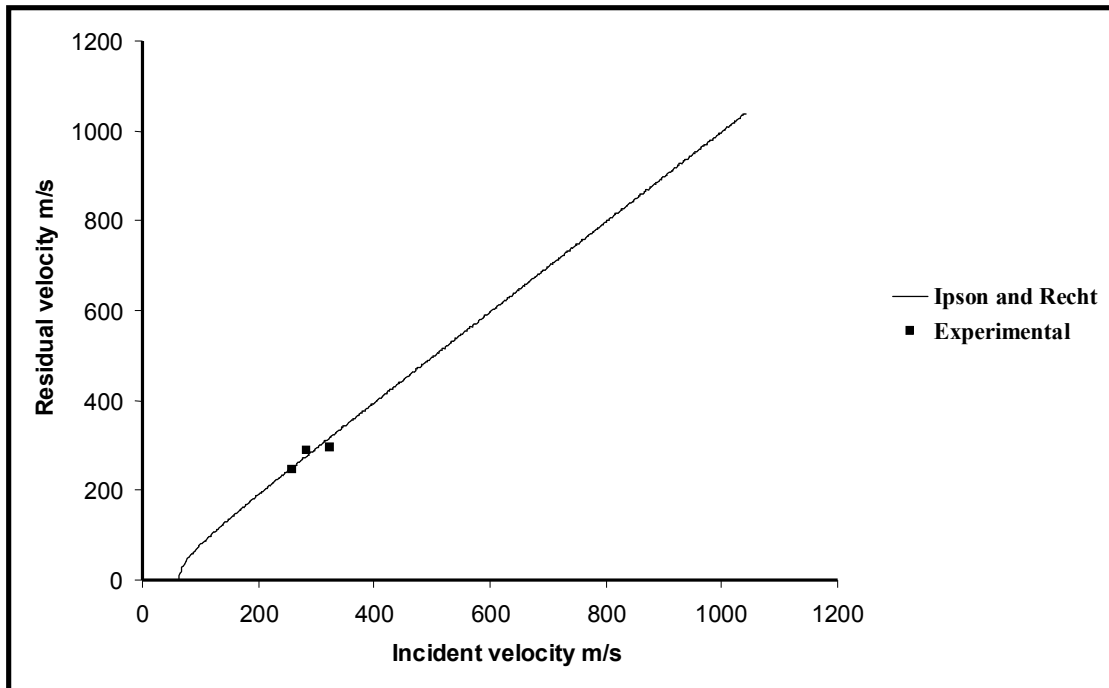


Fig. 8. Final velocity $V(r)$ versus incident velocity $V(i)$ for 4 layer woven composite by hemispherical projectile

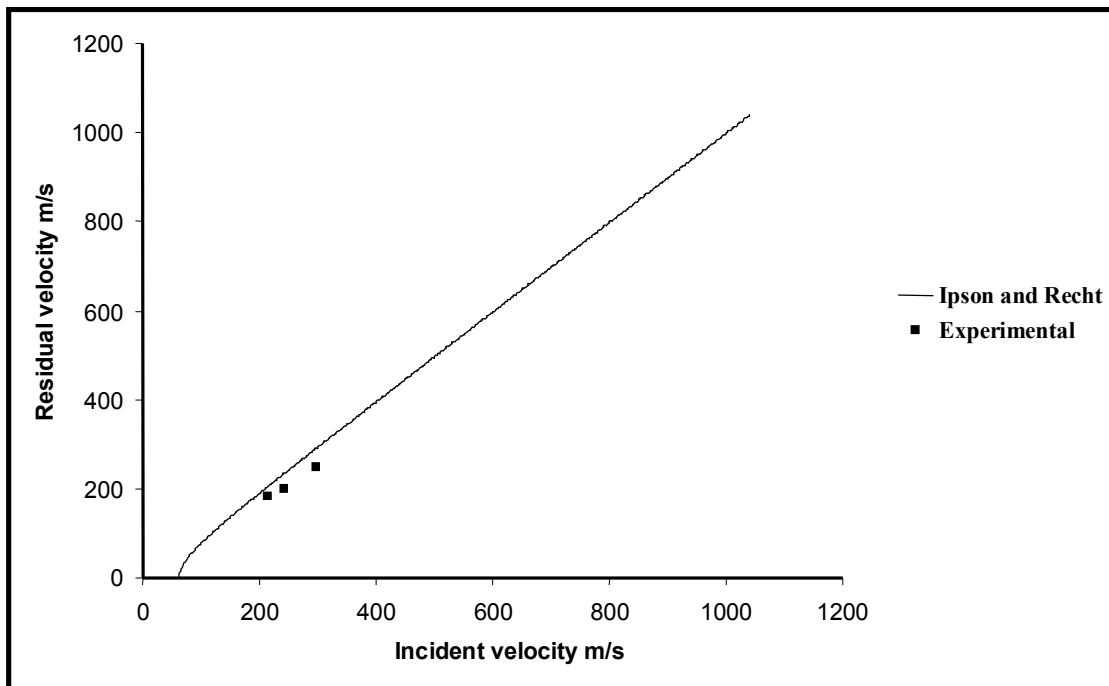


Fig. 9. Final velocity $V(r)$ versus incident velocity $V(i)$ for 6 layer woven composite by hemispherical projectile

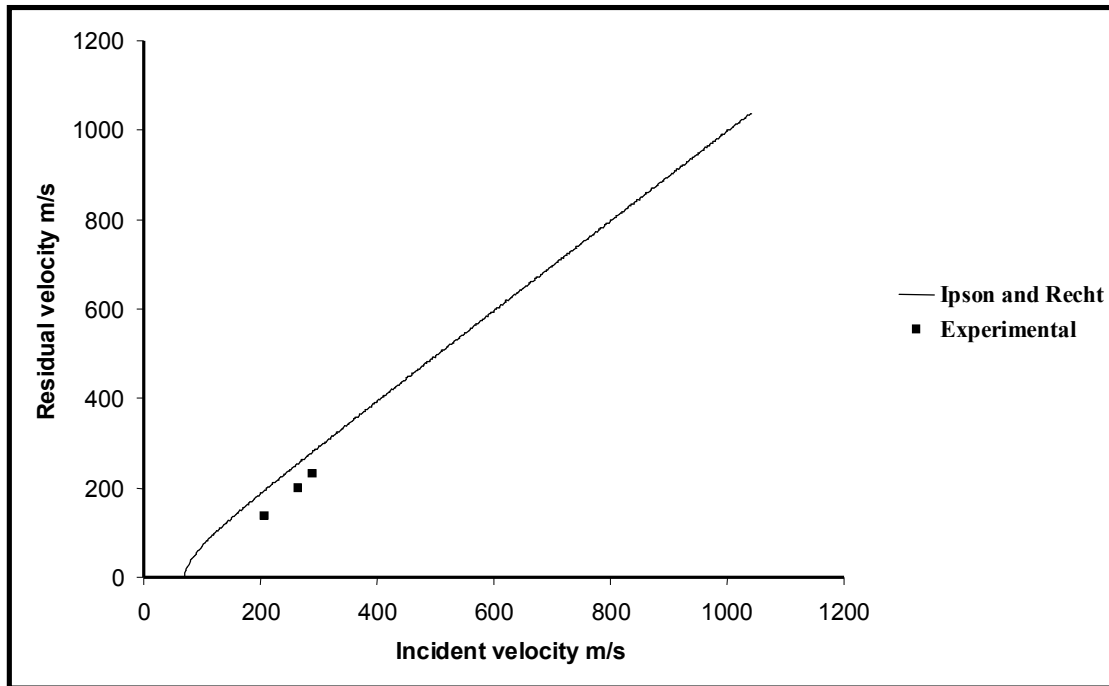


Fig. 10. Final velocity $V(r)$ versus incident velocity $V(i)$ for 8 layer woven composite by hemispherical projectile

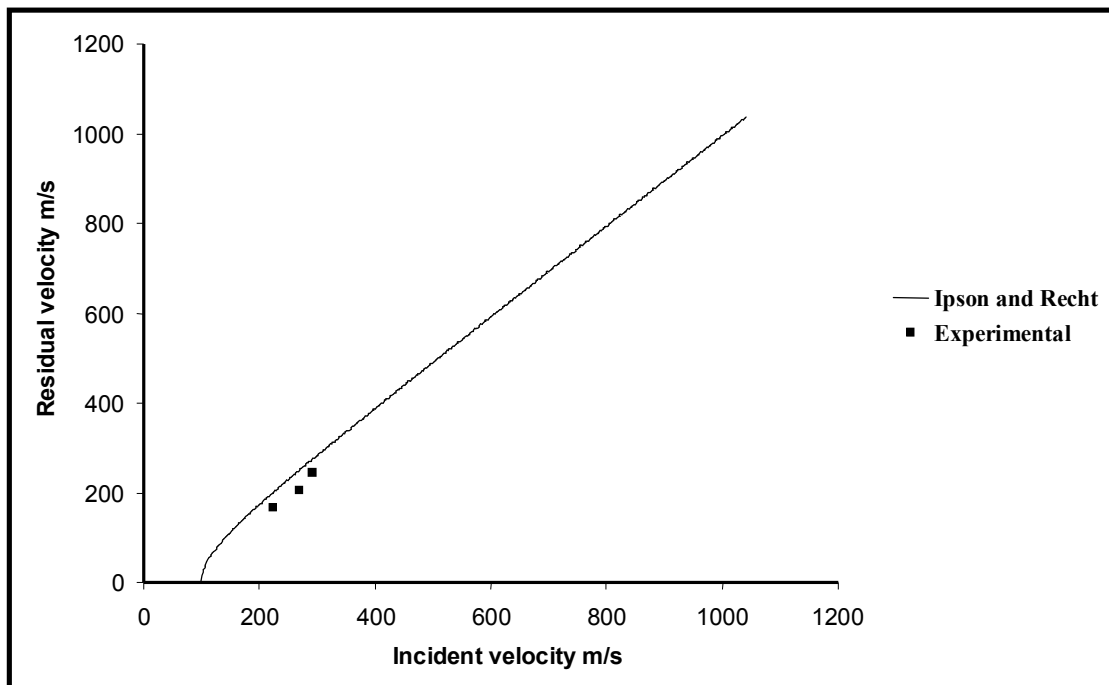


Fig. 11. Final velocity $V(r)$ versus incident velocity $V(i)$ for 10 layer woven composite by hemispherical projectile

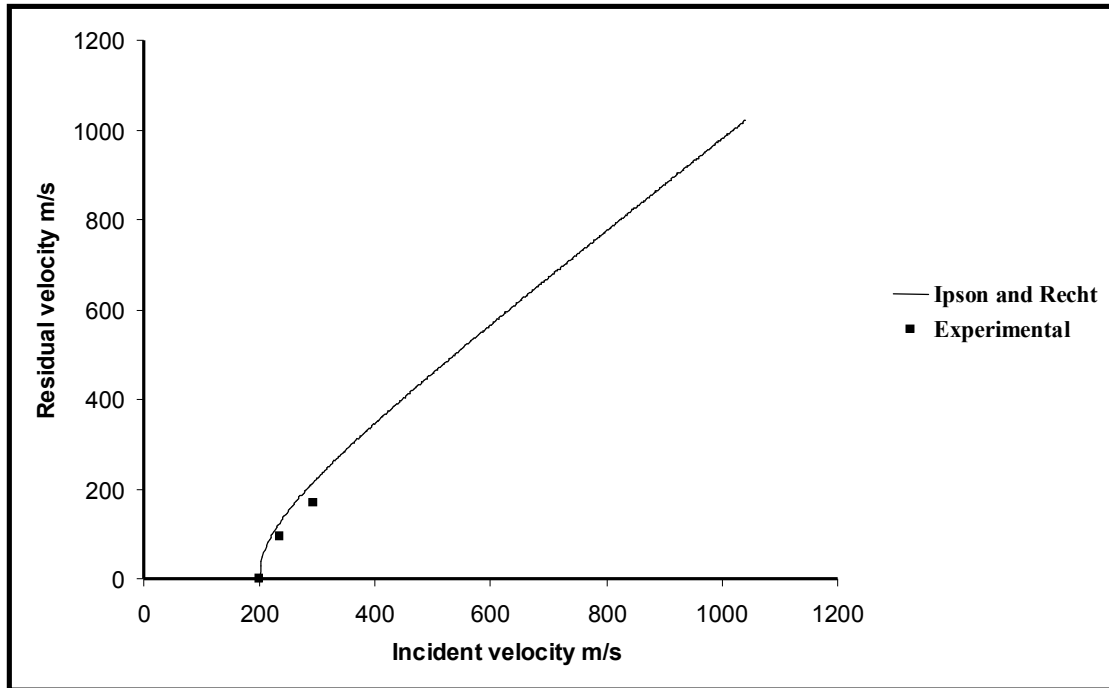


Fig.12. Final velocity $V(r)$ versus incident velocity $V(i)$ for 20 layer woven composite by hemispherical projectile

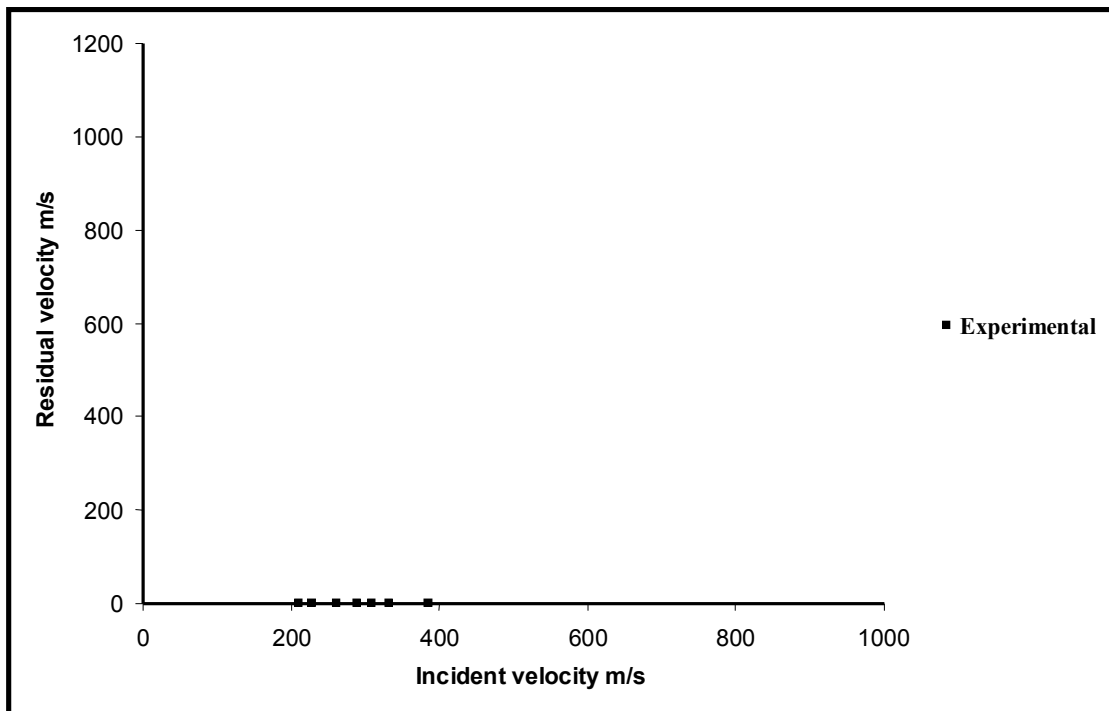


Fig.13. Final velocity $V(r)$ versus incident velocity $V(i)$ for 30 layer woven composite by hemispherical projectile



Fig.14. A cross sectional view of perforated zone composite material target of 20 layer woven fiber Kevlar/ Al_2O_3 powder in a Epoxy matrix struck by a hemispherical projectile as $V_i = 321.78$ m/s



Fig.15. Composite material target of 30 layer woven fiber Kevlar/ Al_2O_3 powder in a Epoxy matrix struck by a hemispherical projectile as $V_i = 385$ m/s



Fig.16. Composite material target of 30 layer woven fiber Kevlar/ Al₂O₃ powder in a Epoxy matrix struck by a hemispherical projectile as $V_i = 390.87$ m/s

Table 1 Comparison between theoretical model ballistic limit velocities with experimental results for ballistic limit velocity

Composite Materials	No. layer Kevlar ²⁹	Thickness (mm)	V _b Theoretically (m/s)	V _b Experimentally (m/s)	Energy Theoretical (J)	Energy Experimental (J)
Kevlar ²⁹ /Al ₂ O ₃	3	2.1	30.4	25.45	2.3	1.6
Kevlar ²⁹ /Al ₂ O ₃	4	3	48.3	51.37	5.83	6.59
Kevlar ²⁹ /Al ₂ O ₃	6	4.35	64.72	61.89	10.47	9.57
Kevlar ²⁹ /Al ₂ O ₃	8	5.4	69.81	73.24	12.18	13.4
Kevlar ²⁹ /Al ₂ O ₃	10	9.67	105.44	99.78	27.79	24.89
Kevlar ²⁹ /Al ₂ O ₃	20	14.23	193.95	200.13	94	100.13
Kevlar ²⁹ /Al ₂ O ₃	30	18	398.2	390.87	396.4	381.9

References

- Abbud, L.H., Talib, A.R.A., Mustapha, F., Tawfique, H., Najim, F.A., 2010, Behaviour of transparent material under high velocity impact. *International Journal of Mechanical and Materials Engineering*; 5:123-128.
- Abu Talib, A.R., L.H. Abbud, A. Ali, F. Mustapha, 2012, Ballistic Impact performance of Kevlar-29 and Al₂O₃ powder/Epoxy Targets under High Velocity Impact. *Materials and Design*; 35: 12-19.
- Andreas, Krell, Thomas Hutzler, Jens Klimke, 2005, Physics and Technology of Transparent Ceramic Armor: Sintered Al₂O₃ vs Cubic Materials. RTO-MP-AVT-122, NATO.
- ASTM D3039/D3039 – 95, 1995, Standard Test Method for Tensile Properties of Polymer Matrix Composite Materials. *Annual Book of ASTM Standards*, Vol. 14.02.

- Boccaccini, A.R., S. Atiq, D.N. Boccaccini, I. Dlouhy, C. Kaya, 2005, Fracture behaviour of mullite fiber reinforced–mullite matrix composites under quasi-static and ballistic impact loading. *Composites Science and Technology*; 65: 325–333.
- Gupta, N.K., M.A. Iqbal, G.S. Sekhon, 2008, Effect of projectile nose shape, impact velocity and target thickness on the deformation behavior of layered plates. *International Journal of Impact Engineering*; 35: 37–60.
- Hetherington, J. G., Energy and Momentum, 1996, Changes During Ballistic Perforation. *International Journal of Impact Engineering*; 18(3): 319-337.
- Kozhushko, A.A., I.I. Rykova, A.B. Sinani, 1991, resistance of ceramics to penetration at impact velocities above 5 Km/s. *Journal de Physique III*; 1: 117-122
- Lo´pez-Puente, J., R. Zaera, C. Navarro, 2008, Experimental and numerical analysis of normal and oblique ballistic impacts on thin carbon/epoxy woven laminates. *Composites: Part A*; 39:374–387.
- Mohamed, Thariq Bin Hameed Sultan, ShahNor bin Basri, Mohammad Saleem, 2007, Prasetyo Edi, High Velocity Impact Analysis of Glass Epoxy-Laminated Plates. Thesis University Putra Malaysia.
- Novotny, W.R., E. Cepus, A. Shahkarami, R. Vaziri, A. Poursartip, 2007, Numerical investigation of the ballistic efficiency of multi-ply fabric armours during the early stages of impact. *International Journal of Impact Engineering*; 34:71–88.
- Pablo, D. Zavattieri and Horatio D. Espinosa, 2000, Ballistic penetration of multi-layered ceramic/steel targets. *American Institute of Physics*; 8: 1117-1120
- Paul, J. Hazell and Michael J. Iremonger, 1998, Damage of ceramic armours subjected to high velocity impact by steel spheres. *Journal of Battlefield Technology*; 1(1): 1-13.
- Recht, R.F. and Ipson, T.W., 1963, Ballistic Perforation Dynamics, *J. Applied Mechanics*, 30: 384 – 390.
- Seigel, A.E. , 1965, The Theory of High Speed Gun. AGARDograph 91, NATO.
- Strassburger E., H. Senf and H. Rothenhausler, 1994, Fracture propagation during impact in three types of ceramics. *Journal de Physique III*; 4: 653-658
- Tan, V.B., T.W. Ching, 2006, Computational simulation of fabric armour subjected to ballistic impacts. *International Journal of Impact Engineering*; 32:1737–1751.
- Teng, X., T. Wierzbicki, M. Huang, 2008, Ballistic resistance of double-layered armor plates. *International Journal of Impact Engineering*; 35: 870–884.
- Teyfik Demir, Mustafa Ubeyli , R.Orhan Yıldırım, 2008, Investigation on the ballistic impact behavior of various alloys against 7.62 mm armor piercing projectile. *Materials and Design*; 29: 2009–2016
- Yadav, S., G. Ravichandran, 2003, Penetration resistance of laminated ceramic/polymer structures. *International Journal of Impact Engineering*; 28:557–574.